



## SELECTION OF OPTIMAL TIME-SCALING FOR THERMOMECHANICAL HYBRID SIMULATION

C.A. Whyte<sup>(1)</sup>, K.R. Mackie<sup>(2)</sup>, G. Abbiati<sup>(3)</sup>, B. Stojadinovic<sup>(4)</sup>

<sup>(1)</sup> Postdoctoral Researcher, Swiss Federal Institute of Technology (ETH) Zürich, [whyte@ibk.baug.ethz.ch](mailto:whyte@ibk.baug.ethz.ch)

<sup>(2)</sup> Associate Professor, University of Central Florida, [kevin.mackie@ucf.edu](mailto:kevin.mackie@ucf.edu)

<sup>(3)</sup> Postdoctoral Researcher, Swiss Federal Institute of Technology (ETH) Zürich, [abbiati@ibk.baug.ethz.ch](mailto:abbiati@ibk.baug.ethz.ch)

<sup>(4)</sup> Professor, Swiss Federal Institute of Technology (ETH) Zürich, [stojadinovic@ibk.baug.ethz.ch](mailto:stojadinovic@ibk.baug.ethz.ch)

### **Abstract**

Mechanics of structural behavior in fire and fire-resistant design of structures are based on data from standard fire tests of single structural components. Experimental qualification of structures in fire must account for interactions between elements within the overall structural assembly in order to provide benchmark tests to verify and validate modeling tools and design provisions, particularly those aiming to implement modern performance-based evaluation approaches and design standards. This is the motivation to extend the hybrid simulation method, which has been deeply investigated in the seismic domain, to structures-in-fire testing. By linking numerical and physical substructures, hybrid simulation offers a flexible, cost-effective approach. However, the implementation of thermomechanical hybrid simulation (TMHS) tests must be carefully designed to properly account for rate-dependent creep effects that become significant at high temperatures. Purely mechanical hybrid simulations are commonly performed at extended time scales. Such an approach is not appropriate in the presence of creep and other loading rate effects: instead, thermomechanical simulation should, ideally, be conducted in real time. However, real-time testing is not always possible due to constraints of the laboratory equipment. In such cases, the testing time scale must be accurately tuned to minimize experimental approximation. The optimal selection of the time integration scale and the numerical integration scheme in TMHS are presented herein. Furthermore, the *thermalTruss* experimental element implemented in the OpenFresco hybrid simulation middleware is presented, which provides the ability to fully simulate a TMHS test prior to experimentally substructuring the physical specimen in the laboratory.

*Keywords: hybrid simulation; thermomechanical; time integration*



## 1. Introduction

Standard fire tests [1, 2, 3], which experimentally examine the response of single structural elements, are not sufficient to understand the behavior of complete structures, and especially not those exposed to complex and dynamic loading scenarios. However, this understanding of global structural behavior is precisely what is needed to develop performance-based standards for fire engineering. Single-component fire tests are commonly utilized because tests of entire structures at large-scale are generally prohibitive, both in terms of time and finances. Given this situation, hybrid simulation (HS) [4, 5, 6], which partitions a hybrid model of a prototype structure into numerical and physical substructures (NSs and PSs, respectively), is the best approach to enable verification and validation of performance-based models for fire engineering of structures. The PSs of the hybrid model are tested in the laboratory because of their strongly nonlinear responses and/or lack of reliable mathematical models, while the NSs are instantiated in structural analysis software. The dynamic response of the hybrid model is solved using a time-stepping response history analysis with reduced costs and effort.

The thermal response time of a typical structure exposed to fire is virtually static compared to the response time of the same structure to dynamic loads, such as earthquakes or explosions. Accordingly, Korzen and co-workers [7] pursued a static force balance during a breakthrough experiment, where they extended HS to fire loads and simulated a steel frame with a single column PS. Later, Mostafaei [8, 9] tested a hybrid model of a 6-story reinforced concrete building with a 3D NS modeled in SAFIR [10] and a single column PS tested in a furnace. At 5-minute time intervals, a human operator adjusted the interface boundary conditions between the NS and PS.

The static approach may not be adequate for simulating the behavior of a structure under fire after an earthquake (and similar load sequences), nor for simulating the dynamics of partial or full collapse of structures under simultaneous fire and mechanical loads, such as those that occur in explosions. In order to study the combined effects of dynamic mechanical loads and fire loads, there was a need for implementing a finite element (FE) code with a transient integrator and automatic data transfer between the substructures as the core solver of the hybrid simulator. With these objectives in mind, Whyte et al. [11] extended the Open-source Framework for Experimental Setup and Control (OpenFresco) [12] middleware to the thermal domain by adding temperature degrees of freedom (DOFs) and thermal control capabilities. They verified and validated the thermomechanical hybrid simulation (TMHS) developments with proof-of-concept tests, using the Open System for Earthquake Engineering Simulation (OpenSees) [13] software framework for modeling the NS.

HS was originally developed for simulating the dynamic structural response to earthquake loads. When a PS is not rate-dependent, as is often the case for a standard structural element in such a purely mechanical HS test, the test is often performed with an extended, pseudodynamic (PsD), time scale that is slower than real-time (RT). The optimal testing time scale is determined by considering the oil flow limitations in the hydraulic power network, the actuator control accuracy, and the synchronization among computational and experimental drivers in the laboratory [14]. In HS tests that also include fire loads, the choice of testing time scale becomes more complicated. When a structure is subjected to high temperatures such that significant creep strains are induced [15], the response of the structure depends on the load rate (in this case, the fire load rate), which necessitates a RT-HS. However, the limits of the laboratory equipment may make it impossible to conduct a RT test. A compromise, in terms of understanding the effects of time-scale distortion in a partial similitude model, similar to the ones made in reduced-scale mechanical tests, is needed to perform a test at all. Regarding the time-scale selection for TMHS, the trade-off is between the simulation accuracy (RT is necessary for perfectly capturing rate-dependent effects) and the laboratory testing capacity. From this perspective, this paper demonstrates, through a series of simulations, the time-scale and numerical integration algorithm selection process in the TMHS test campaign conducted by Whyte et al. [11], aimed at minimizing the model distortions and optimizing the accuracy of the TMHS under the given equipment constraints. Furthermore, modifications to the TMHS experimental element in OpenFresco are presented that allow full simulation of a TMHS test prior to designing and implementing the PS in the laboratory.



## 2. Substructuring of the Thermoelastic Equations

The thermomechanical substructuring framework is introduced in Eq. (1) for a generic spatially discretized thermoelastic system [16]:

$$\begin{bmatrix} M_{uu} & 0 \\ 0 & 0 \end{bmatrix} \begin{bmatrix} \ddot{u} \\ \ddot{\theta} \end{bmatrix} + \begin{bmatrix} C_{uu} & 0 \\ 0 & C_{\theta\theta} \end{bmatrix} \begin{bmatrix} \dot{u} \\ \dot{\theta} \end{bmatrix} + \begin{bmatrix} K_{uu} & K_{u\theta} \\ 0 & K_{\theta\theta} \end{bmatrix} \begin{bmatrix} u \\ \theta \end{bmatrix} = \begin{bmatrix} F_u \\ F_\theta \end{bmatrix} \quad (1)$$

The matrix partitioning refers to displacement and temperature DOFs,  $u$  and  $\theta$ , respectively, and their derivatives.  $M_{uu}$ ,  $C_{uu}$ , and  $K_{uu}$  are the mass, damping, and stiffness matrices.  $K_{\theta\theta}$  and  $C_{\theta\theta}$  are the heat conduction and capacity matrices.  $F_u$  and  $F_\theta$  are the mechanical external forces and the thermal fluxes. Positive thermal fluxes supply power to the system. Because the off-diagonal sub-matrix,  $K_{u\theta}$ , represents the internal forces due to thermal deformations, its inclusion is crucial to account for TM structural interactions. As shown in Eq. (2), by applying the HS technique, each matrix can be split into numerical (N) and physical (P) components.

$$\begin{aligned} & \begin{bmatrix} (M_{uu}^N + M_{uu}^P) & 0 \\ 0 & 0 \end{bmatrix} \begin{bmatrix} \ddot{u} \\ \ddot{\theta} \end{bmatrix} + \begin{bmatrix} (C_{uu}^N + C_{uu}^P) & 0 \\ 0 & (C_{\theta\theta}^N + C_{\theta\theta}^P) \end{bmatrix} \begin{bmatrix} \dot{u} \\ \dot{\theta} \end{bmatrix} \\ & + \begin{bmatrix} (K_{uu}^N + K_{uu}^P) & (K_{u\theta}^N + K_{u\theta}^P) \\ 0 & (K_{\theta\theta}^N + K_{\theta\theta}^P) \end{bmatrix} \begin{bmatrix} u \\ \theta \end{bmatrix} = \begin{bmatrix} F_u^N + F_u^P \\ F_\theta^N + F_\theta^P \end{bmatrix} \end{aligned} \quad (2)$$

The first row block of Eq. (2) represents the equation of motion of the system, whilst the second row block describes the heat transfer problem. In the case of a cold NS (i.e. no thermal loads are applied to the NS), the heat transfer problem is confined to the PS, and therefore only the equation of motion enters the time stepping scheme of the hybrid simulator. Then, a classical mechanical time stepping algorithm is sufficient to conduct the test. In the PsD case with a cold NS, rate-dependent components of the PS restoring force are simulated numerically, and the system of equations defined by Eq. (2) reduces to Eq. (3).

$$\begin{aligned} & (M_{uu}^N + M_{uu}^P) \ddot{u} + (C_{uu}^N + C_{uu}^P) \dot{u} + K_{uu}^N u = F_u^N - R_u^P \\ & R_u^P = K_{uu}^P u + K_{u\theta}^P \theta - F_u^P \end{aligned} \quad (3)$$

On the other hand, in the RT case with a cold NS, the system of equations in Eq. (4) holds.

$$\begin{aligned} & M_{uu}^N \ddot{u} + C_{uu}^N \dot{u} + K_{uu}^N u = F_u^N - R_u^P \\ & R_u^P = M_{uu}^P \ddot{u} + C_{uu}^P \dot{u} + K_{uu}^P u + K_{u\theta}^P \theta - F_u^P \end{aligned} \quad (4)$$

## 3. Description of the Proof-of-Concept Case Study

The hybrid model used for the TMHS proof-of-concept tests of Whyte and co-workers [11] is retained for the simulations presented in this paper. The prototype structure is a long-span girder fixed at both ends and supported at mid-span by a hanger exposed to a fire. By utilizing symmetry, one half of the prototype girder (NS) and one half of the prototype hanger (PS) comprise the scaled hybrid model, shown in Fig. 1.

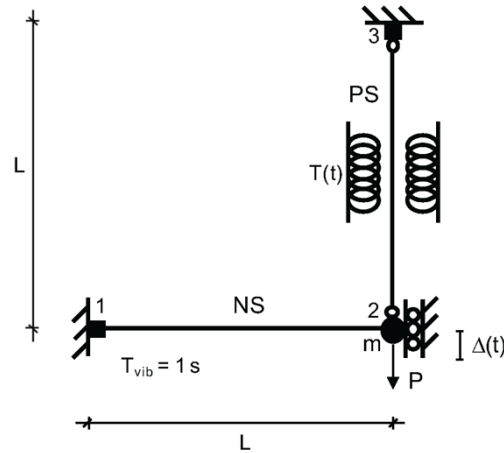


Fig. 1 – Hybrid model

The vertical displacement at node 2 is the single free DOF of the hybrid model. The steel beam NS is assumed to be insulated from the fire and from the PS, so it is modeled as an unheated *elasticBeamColumn* element in OpenSees. The steel truss PS is modeled using the recently developed OpenFresco *thermalTruss* experimental element. In the basic coordinate system, this experimental element has one mechanical DOF (element elongation) and two temperature DOFs (one at each node). The cross-sectional dimensions of the PS are 9.78 mm x 3.31 mm, and the length is  $L = 40$  mm. The Young's modulus of the steel material,  $E = 200$  GPa. The steel coefficient of thermal expansion,  $\alpha = 10 \times 10^{-6}$  m/m/°C, is estimated from preliminary TMHS data. The numerical mass, applied to node 2, is selected to obtain the vibration period of the hybrid model  $T_n = 1$  s. The cross-sectional moment of inertia of the NS and the mechanical and thermal load ranges are chosen such that the PS remains linear elastic, and that significant changes in steel mechanical parameters due to temperature variations do not occur. The mechanical tensile force,  $P(t)$ , is applied at node 2 (Fig. 1) as a linear load ramp from 0 to 15 kN. Simultaneously, the surface temperature of the PS is heated in the furnace with a scaled version of the international standard ISO 834 temperature-time fire curve, as defined in Eurocode 1 Part 1-2 [17], and as shown in Eq. (5):

$$T(t) = 20 + 345 \log_{10}(8t + 1) \quad (5)$$

where  $T(t)$  is temperature [°C] in the fire compartment and  $t$  is time [min]. A scaling factor multiplies  $T(t)$  and is adjusted with respect to the starting room temperature so that a final temperature of 200°C is achieved at the end of the TMHS test. All of the following simulations refer to this benchmark case study.

#### 4. Optimization of the Testing Time Scale and Numerical Integration Scheme

The testing time scale,  $\lambda$ , is defined as shown in Eq. (6).

$$\lambda = \frac{dt_{sim}}{dt_{int}} \quad (6)$$

Here,  $dt_{sim}$  is the wall-clock time required to complete one analysis time step in the laboratory, and  $dt_{int}$  is the numerical integration time step length.  $\lambda=1$  in a RT-HS, and  $\lambda>1$  in a PsD HS.

Increasing the testing time scale, resulting in a HS that proceeds slower than RT, is acceptable when the restoring force measured from the PS is rate-independent. However, when the restoring force measured from the PS is rate-dependent, such as in the case of specimen creep in high temperature tests, increasing the testing time



scale distorts the results. This is especially significant for fire tests because they tend to be quite long. For example, in the final Cardington test [18], the maximum steel temperature occurred after 57 min, and the duration of the test was 150 min. Even with a small TMHS testing time scale of  $\lambda = 2$ , a 150 min test would last 300 min and could significantly bias the results.

As can be observed in Eq. (6), a reduction of the testing time scale can be achieved by reducing  $dt_{sim}$  or increasing  $dt_{int}$ . Therefore, the combination of the lower bound of  $dt_{sim}$  and the upper bound of  $dt_{int}$  dictate the minimum allowable, and thus most preferential, testing time scale. In particular,  $dt_{sim}$  relates to the performance of the experimental and the computational equipment, and can be reduced by increasing the communication network speed, reducing the actuation delay, or boosting the computational driver [6]. On the other hand, the maximum allowable  $dt_{int}$  is limited by the stability and accuracy criteria of the selected numerical integration method [19].

In the present case study, the minimum value for  $dt_{sim}$  allowed by the experimental setup in the laboratory is 6 s, due to the slow reaction time of the furnace. The size of  $dt_{int}$  and the selection of numerical integration scheme are established by the following series of purely numerical simulations and corresponding error analyses. A simple linear elastic model is developed in Matlab to simulate the thermomechanical response of the hybrid model (Fig. 1). The model simulates the effect of PS elongation due to thermal expansion and the noise observed in the force feedback signal. The thermal elongation is calculated using Eq. (7):

$$u_{th} = \alpha \Delta T L \quad (7)$$

where  $\alpha$  [m/m/°C] is the coefficient of thermal expansion,  $\Delta T$  is the difference between the current temperature and the initial temperature, and  $L$  is the length of the specimen. For the hot-rolled steel specimens used in the hybrid tests, creep starts to become significant at about 400°C [20]. Because these proof-of-concept tests remain at relatively low temperatures (up to 200°C), creep is not yet a concern and does not have to be considered in the model. Gaussian noise with a root mean square (RMS) value of 50 N is added to the restoring force to simulate measurement errors. This is measured from preliminary TMHS test results, and is significantly smaller than the maximum 15 kN load applied to the hybrid model.

The thermomechanical response of the hybrid model is simulated in Matlab using 5 integration schemes: the explicit variant of the Newmark algorithm [21], the implicit variant of the Newmark algorithm [21], the Alpha Operator-Splitting (Alpha OS) algorithm with  $\alpha = 0.9$  [22], the Wilson Theta algorithm with  $\theta = 1.4$  [23], and the Houbolt algorithm [23]. For the explicit algorithm, the upper bound of  $dt_{int}$  is further constrained by the stability limit and is equal to  $T_n/\pi = 0.32$  s. All other algorithms are implicit and unconditionally stable.

A reference solution is obtained considering a sufficiently small integration time step,  $dt_{int} = 0.01$  s, and no restoring force noise. RMS errors between the displacement history of the TMHS simulation and the reference solution are calculated for a range of  $dt_{int}$  between 0.01 s and 0.3 s and averaged over 1000 simulations. The values obtained are normalized by the difference between the maximum and minimum displacement values of the reference solution and are presented in Fig. 2.

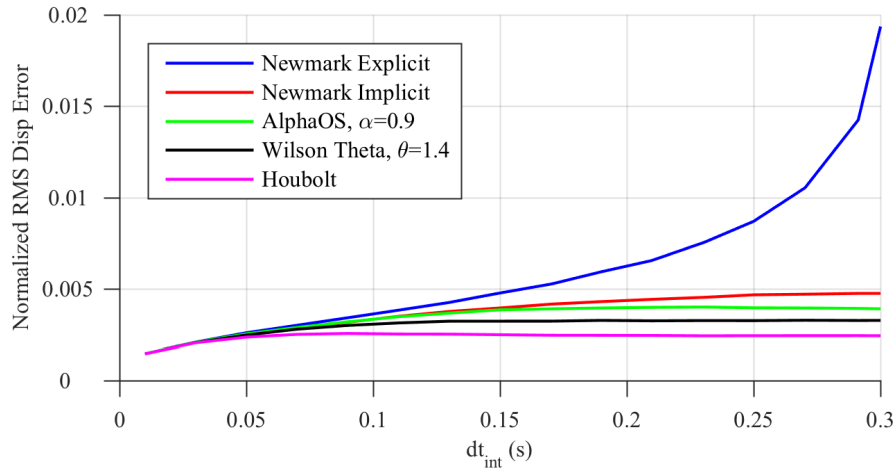


Fig. 2 – Normalized RMS error curves of hybrid model response for a range of dt sizes

As can be appreciated from Fig. 2, the normalized RMS error remains small even for coarse integration time step values. This can be intuitively justified by the quasi-static character of the hybrid model response. As a result,  $dt_{int} = 0.25$  s is selected for conducting the HS tests, which gives satisfactorily small error values. The explicit and implicit variations of the Newmark algorithm have been experimentally tested to date. Together with  $dt_{sim} = 6$  s, a testing time scale of  $\lambda = 24$  is obtained. The Alpha OS, Wilson Theta, and Houbolt integration schemes, which include algorithmic damping, show slightly improved performance over the Newmark Implicit scheme.

Using the selected  $dt_{int} = 0.25$  s, the performance of the numerical integrators is investigated with varying amounts of noise added to the restoring force signal. Fig. 3 shows the normalized RMS displacement errors for restoring Gaussian noise RMS values ranging from 0 to 400 N. This data is processed the same way as the data for varying the integration time step size. Average RMS errors are found over 1000 simulations.

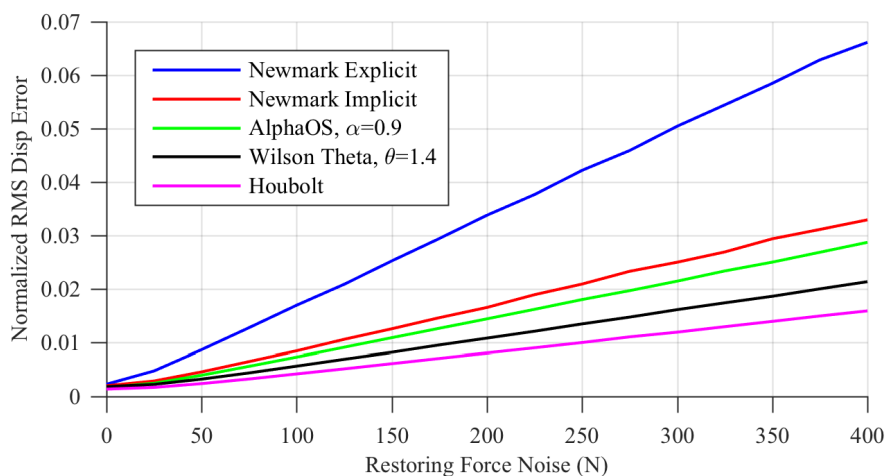


Fig. 3 – Normalized RMS error curves of hybrid model response for a range of restoring force noise magnitudes

In Fig. 3, the numerical integration schemes with algorithmic damping are shown to slightly reduce the RMS errors. As the amount of restoring force noise is increased, the integration schemes with algorithmic damping

become even more effective (the lines on the plot are diverging). This result shows promise for implementing algorithmic damping schemes in future TMHS tests.

## 5. OpenFresco TMHS Experimental Element

In order to enable TMHS in OpenFresco, a *thermalTruss* experimental element has been recently implemented [11] with the following syntax:

```
expElement thermalTruss $tag $iNode $jNode -site $siteTag <-alpha $alphaVal> -initStif $K <-iMod> <-rho $rho>
```

For a TMHS, the optional thermal expansion parameter, *alpha*, should not be used. When *alpha* is included, this triggers the *thermalTruss* experimental element to work in a numerical simulation mode in conjunction with *SimUniaxialMaterials* experimental control [24]. This experimental control accepts a target displacement and returns a simulated force response based on an assigned OpenSees material model. With the numerical simulation mode, it is possible to fully simulate a TMHS prior to laboratory implementation including the effect of the middleware.

The simulated TMHS works as follows. In the proof-of-concept test, the specimen is moved mechanically in tension through displacement control. The thermal expansion also serves to further elongate the specimen. When the equation of motion is solved for a target displacement in each time step, this is a total target displacement  $u_{total}$ . It is comprised of a mechanical displacement,  $u_m$ , portion and a thermal displacement,  $u_{th}$ , portion. As the temperature increases,  $u_{th}$  increases and  $u_m$  correspondingly decreases. Therefore, when *alpha* is included to trigger the simulation mode, the experimental element calculates the displacement due to thermal strain,  $u_{th}$ , in each step using Eq. (7). Then,  $u_{th}$  is subtracted from the command displacement. The resulting updated command displacement is passed to the OpenFresco *SimUniaxialMaterials* experimental control, which returns a simulated force. This implementation has been validated with Matlab simulations and the proof-of-concept test results. Fig. 4 compares the displacement and force responses of the hybrid system obtained from the TMHS experiments with those simulated in OpenFresco and Matlab using the same simulation parameters as presented in the previous sections.

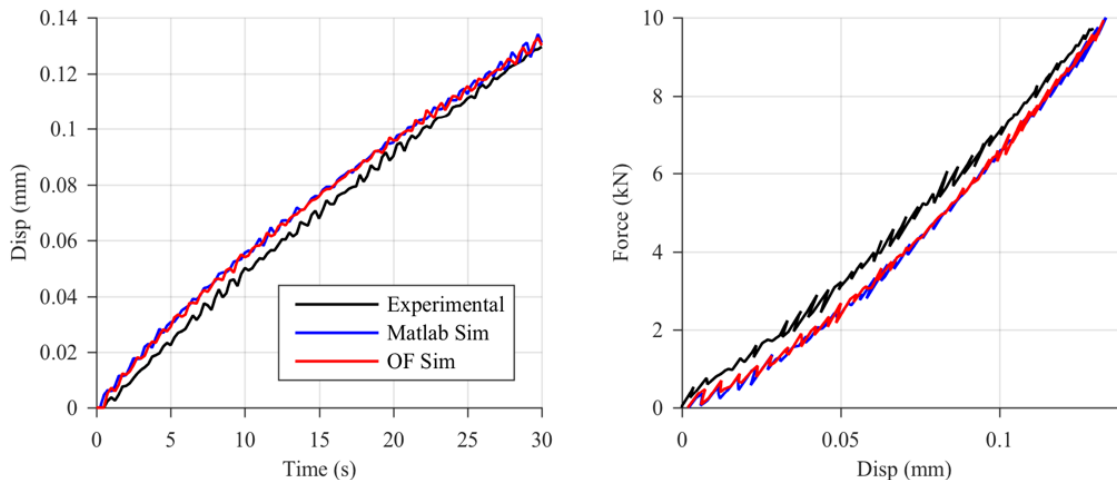


Fig. 4 – Validation of the OpenFresco thermalTruss element

As can be appreciated from Fig. 4, the OpenFresco simulation matches the Matlab simulation, and both models agree very well with the experimental test.



## 5. Conclusions

The hybrid simulation technique, which originated for studying the dynamic response of structures to earthquake ground motion excitation, has been recently enhanced to combine mechanical and thermal loads. The thermomechanical hybrid simulation paradigm offers insight into the responses of large and complex structural systems subjected to both mechanical and fire loadings. In this context, particular care must be devoted to the proper selection of the testing time scale. When high temperature and long duration thermal loads are involved, rate-dependent material creep becomes a concern and restricts the use of extended simulation time scales. While real-time tests would be ideal in these situations, laboratory equipment is often not capable of attaining real-time speeds. As a result, the optimal testing time scale is a trade-off between simulation accuracy and testing capacity.

To investigate this problem, a simple linear elastic model was developed in Matlab to determine the appropriate size of numerical integration time step,  $dt_{int}$ , and the choice of numerical integration algorithm. Through these simulations,  $dt_{int} = 0.25$  s was selected. Together with  $dt_{sim} = 6$  s, a testing time scale of  $\lambda = 24$  was obtained, and the explicit and implicit variations of the Newmark algorithm have been experimentally tested. The simulations show that the following integration schemes with algorithmic damping, Alpha OS, Wilson Theta, and Houbolt, are beneficial for reducing the hybrid simulation errors that result from noise in the force feedback signal. Future experimental campaigns will incorporate these integrators. For the TMHS tests to 200°C, which do not involve significant specimen creep, the testing time scale of  $\lambda = 24$  is acceptable. When high temperature tests are performed, the testing time scale will have to be reduced through improving the performance of the furnace in order to produce simulation results that have an acceptable accuracy.

A recently developed OpenFresco *thermalTruss* experimental element allows full numerical simulation of a TMHS prior to implementation in the laboratory. This element enables evaluation of the suitability of experimental approximations, and is of paramount importance for validating hybrid simulation test settings before laboratory implementation. Future developments will include the possibility to simulate physical substructures with rate-dependent behavior.

## 6. References

- [1] Dwaikat MMS, Kodur VKR, Quiel SE, Garlock MEM (2011): Experimental behavior of steel beam-columns subjected to fire-induced thermal gradients. *Journal of Construction Steel Research*, **67** (1), 30-38.
- [2] Martins AMB, Rodrigues JPC (2010): Fire resistance of reinforced concrete columns with elastically restrained thermal elongation. *Engineering Structures*, **32** (1), 3330-3337.
- [3] Tondini N, Rossi B, Franssen JM (2013): Experimental investigation on ferritic stainless steel columns in fire, *Fire Safety Journal*, **62**, 238-248.
- [4] Takanashi K, Udagawa K, Seki M, Okada T, Tanaka H (1975): Non-linear earthquake response analysis of structures by a computer-actuator on-line system, *Bulletin of Earthquake Resistant Structure Research Center*, Institute of Industrial Science, University of Tokyo, Tokyo.
- [5] Mahin SA, Williams ME (1981): Computer controlled seismic performance testing, 2<sup>nd</sup> ASCE-EMD Specialty Conference on Dynamic Response of Structures, Atlanta, USA.
- [6] Stojadinovic B, Mosqueda G, Mahin SA (2006): Event-Driven Control System for Geographically Distributed Hybrid Simulation, *ASCE Journal of Structural Engineering*, **132** (1), 68-77.
- [7] Korzen M, Magonette G, Buchet P (1999): Mechanical loading of columns in fire tests by means of the substructuring method, *Zeitschrift für Angewandte Mathematik und Mechanik*, **79**, S617-S618.
- [8] Mostafaei H (2013): Hybrid fire testing for assessing performance of structures in fire – Application, *Fire Safety Journal*, **56**, 30–38.



- [9] Mostafaei H (2013): Hybrid fire testing for assessing performance of structures in fire – Methodology, *Fire Safety Journal*, **58**, 170–179.
- [10] Franssen JM et al (1995): A simple model for the fire resistance of axially-loaded members according to Eurocode 3, *Journal of Construction Steel Research*, **35** (1), 49-69.
- [11] Whyte CA, Mackie KR, Stojadinovic B (2016): Hybrid Simulation of Thermomechanical Structural Response, *Journal of Structural Engineering*, **142** (2), 04015107-1 – 04015107-11.
- [12] OpenFresco (2016): Open Framework for Experimental Setup and Control. <<http://openfresco.neesforge.nees.org>> (9 May 2016).
- [13] OpenSees (2016): Open System for Earthquake Engineering Simulation. <<http://opensees.berkeley.edu>> (9 May 2016).
- [14] Bursi OS, Wagg D, eds. (2008): Modern testing techniques for structural systems, International Centre for Mechanical Sciences, *CISM Courses and Lectures*, 502, Springer.
- [15] Anderberg Y (1988): Modelling steel behavior, *Fire Safety Journal*, **13** (1), 17-26.
- [16] Hetnarski RB, Eslami MR, Gladwell GML (2009): Thermal stresses: advanced theory and applications, **41**, Springer.
- [17] CEN (European Committee for Standardization) (2002): Eurcode 1: Actions on structures – Part 1-2: General actions – Actions on structures exposed to fire, *EN1991-1-2*, Brussels, Belgium.
- [18] Wald F et al (2006): Experimental behavior of a steel structure under natural fire, *Fire Safety Journal*, **41** (7), 509-522.
- [19] Griffiths D, Griffiths H, Desmond, J (2010): Numerical Methods for Ordinary Differential Equations: Initial Value Problems, Springer Science and Business Media.
- [20] Anderberg Y (1983): Behaviour of steel at high temperatures, *Rilem-Committee 44-PHT*, Lund Institute of Technology, Sweden.
- [21] Newmark NM (1959): A method of computation for structural dynamics, *Journal of Engineering Mechanics*, ASCE, **85** (EM3), 67-94.
- [22] Nakashima M, Kaminosono T, Ishida M, Ando K (1990): Integration techniques for substructure pseudo dynamic test, *4<sup>th</sup> US National Conference on Earthquake Engineering*, Palm Springs, USA.
- [23] Gladwell I, Thomas R (1980): Stability properties of the Newmark, Houbolt, and Wilson Theta methods, *International Journal for Numerical and Analytical Methods in Geomechanics*, **4**, 143-158.
- [24] Schellenberg A, Mahin S, Fenves G (2009): Advanced implementation of hybrid simulation, *Technical Report PEER 2009/104*, Pacific Earthquake Engineering Research, Berkeley, USA.